Biomedical Optics EXPRESS

Dual tree complex wavelet transform based denoising of optical microscopy images

Ufuk Bal

Faculty of Technology, Muğla Sıtkı Koçman University, 48000 Kötekli/Muğla, Turkey
ufukbal@mu.edu.tr

Abstract: Photon shot noise is the main noise source of optical microscopy images and can be modeled by a Poisson process. Several discrete wavelet transform based methods have been proposed in the literature for denoising images corrupted by Poisson noise. However, the discrete wavelet transform (DWT) has disadvantages such as shift variance, aliasing, and lack of directional selectivity. To overcome these problems, a dual tree complex wavelet transform is used in our proposed denoising algorithm. Our denoising algorithm is based on the assumption that for the Poisson noise case threshold values for wavelet coefficients can be estimated from the approximation coefficients. Our proposed method was compared with one of the state of the art denoising algorithms. Better results were obtained by using the proposed algorithm in terms of image quality metrics. Furthermore, the contrast enhancement effect of the proposed method on collagen fiber images is examined. Our method allows fast and efficient enhancement of images obtained under low light intensity conditions.

OCIS codes: (100.0100) Image processing; (100.7410) Wavelets; (100.3020) Image reconstruction-restoration.

References and links

1. S. Delpretti, F. Luisier, S. Ramani, T. Blu, and M. Unser, "Multiframe sure-let denoising of timelapse fluorescence microscopy images," in *5th IEEE International Symposium on Biomedical Imaging: from Nano to Macro, 2008. ISBI 2008* (IEEE, 2008), pp. 149–152.
2. C. Vonesch, F. Aguet, J. L. Vonesch, and M. Unser, "The colored revolution of bioimaging," IEEE Signal Process. Mag. **23**(3), 20–31 (2006).
3. Q. Wu, F. A. Merchant, and K. R. Castleman, *Microscope Image Processing* (Academic, Amsterdam, 2008).
4. F. Luisier, T. Blu, and M. Unser, "Image denoising in mixed Poisson-Gaussian noise," IEEE Trans. Image Process. **20**(3), 696–708 (2011).
5. F. J. Anscombe, "The transformation of Poisson, binomial and negative-binomial data," Biometrika **35**, 246–254 (1948).
6. D. L. Donoho, "Nonlinear wavelet methods for recovery of signals, densities, and spectra from indirect and noisy data," in *Proceedings of Symposia in Applied Mathematics. Vol 47. Different Perspectives on Wavelets*, I. Daubechies, ed. (American Mathematical Society, 1993).
7. D. Donoho, "De-noising by soft-thresholding," IEEE Trans. Inf. Theory **41**(3), 613–627 (1995).
8. P. Fryzlewicz and G. P. Nason, "A Haar-Fisz algorithm for Poisson intensity estimation," J. Comput. Graph. Statist. **13**(3), 621–638 (2004).
9. F. Luisier, C. Vonesch, T. Blu, and M. Unser, "Fast interscale wavelet denoising of Poisson-corrupted images," Signal Process. **90**(2), 415–427 (2010).
10. I. W. Selesnick, R. G. Baraniuk, and N. C. Kingsbury, "The dual-tree complex wavelet transform," IEEE Signal Process. Mag. **22**(6), 123–151 (2005).
11. N. Kingsbury, "The dual-tree complex wavelet transform: a new efficient tool for image restoration and enhancement," in *Proceedings of the 9th European Signal Processing Conference (EUSIPCO 98)*, (Typorama, 1998), pp. 319–322.
12. F. Daniels, "Quantification of collagen orientation in 3D engineered tissue," in *Biomedical Engineering* (Eindhoven University of Technology, Eindhoven, 2006).
13. N. Kingsbury, "The dual-tree complex wavelet transform: a new technique for shift invariance and directional filters," in *Proceedings of the 8th IEEE DSP Workshop, Utah* (IEEE, 1998), Vol. 8, p. 86
14. V. Musoko, "Biomedical signal and image processing," in *Computing and Control Engineering* (Institute of Chemical Technology, Prague, 2005).

#173666 - $15.00 USD Received 1 Aug 2012; revised 7 Nov 2012; accepted 9 Nov 2012; published 13 Nov 2012

15. A. Salih Husain and S. Aymen Dawood, "Image compression based on 2D dual tree complex wavelet transform," Eng. Technol. J. **28**, 1290–1305 (2010).
16. H. M. Salinas and D. C. Fernández, "Comparison of PDE-based nonlinear diffusion approaches for image enhancement and denoising in optical coherence tomography," IEEE Trans. Med. Imaging **26**(6), 761–771 (2007).

1. Introduction

In optical imaging there exist several noise sources such as electronic thermal noise, background noise, readout noise and photon shot noise [1]. Signal independent noise contributions (e.g., electronic thermal noise, background noise, readout noise) can be considered as normally distributed. However live samples are often observed at very low light levels, due to acquisition-time and photobleaching constraints [2]. In this case photon shot noise, which results from the random nature of photon emission, is the major source of noise in optical imaging. Photon shot noise, which is signal dependent, can be characterized by a Poisson distribution [3].

There are several wavelet based denoising methods applicable for optical microscopy when noise is described by a Poisson process [4]. One approach consists in "Gaussianizing" the Poisson measurements. This usually relies on a non-linear preprocessing of the data to stabilize the variance [5,6]. After "stabilization", any high-quality AWGN (additive white Gaussian noise) denoiser can be applied. In general, denoising methods for AWGN reduction based on the wavelet transform consist of three steps: 1) calculation of the wavelet transform of the noisy image (decomposition), 2) modification the wavelet coefficients according to some rule (thresholding), and 3) calculation of the inverse transform using the modified wavelet coefficients (reconstruction). Main assumption of this type of denoising (thresholding) is small coefficients are dominated by noise, while coefficients with a large absolute value carry more signal information than noise. Thresholding may be global or level dependent, hard or soft, based on a priori known or estimated noise statistics [7].

For Poisson noise reduction, beyond "stabilization" there exist different approaches which use the fact that the unnormalized Haar wavelet transform has the remarkable property of preserving Poisson statistics in its lowpass channel [8]. For instance PURE-LET (Poisson Unbiased Risk Estimate-Linear Expansion of Thresholds), is based on the minimization of an unbiased estimate of the MSE (Mean Square Error) for Poisson noise and the preservation of Poisson statistics across scales within the Haar DWT (Discrete Wavelet Transform) [9].

Although DWT has been successfully used for image denoising, it has shortcomings such as shift variance, aliasing and lack of directionality [10]. To overcome these limitations DT-CWT (Dual Tree Complex Wavelet Transform) is introduced [11]. In our proposed denoising algorithm, test images are decomposed using DT-CWT and soft thresholding is applied to the wavelet coefficients. Using similar approach as PURE-LET method we determined threshold values for wavelet coefficients based on approximation coefficients at the same scale.

Unlike other test images we evaluated performance of our algorithm on collagen images by CNR (Contrast to Noise Ratio) metric. The quality of the collagen fiber images from the TPLSM (Two Photon Laser Scanning Microscopy) is poor [12]. For this type of images denoising may blur fibers, making them harder to detect. Our proposed method preserves edges while reducing noise substantially.

2. Materials and methods

2.1. Dual tree complex wavelet transform

For the DWT small changes in the input may cause large changes in the wavelet coefficients. Furthermore aliasing occurs due to downsampling. Inverse DWT cancels this aliasing provided if the wavelet and scaling coefficients are not changed (e.g., noise, thresholding) [10]. The other disadvantage of DWT is its poor directional selectivity (e.g., inability to distinguish between +45° and –45° spectral features). These problems of Real DWT can be

#173666 - $15.00 USD Received 1 Aug 2012; revised 7 Nov 2012; accepted 9 Nov 2012; published 13 Nov 2012

solved using complex wavelets. However, a further problem arises in achieving perfect reconstruction for complex wavelet decomposition beyond level 1. To overcome this, Kingsbury proposed the DT-CWT, which allows perfect reconstruction while still providing the other advantages of complex wavelets [13].

The DT-CWT uses analytic filters to perform the wavelet analysis. It uses two Real DWT trees to implement its real (tree a) and imaginary (tree b) parts. DT-CWT decomposes a signal in terms of a complex shifted and dilated mother wavelet ψ(x) and scaling function φ(x). The real (r) and imaginary (i) parts of the wavelet and scaling functions for one dimensional case can be described as

$$\psi_r(t) = \sqrt{2}\sum_n H_a(n)\varphi_r(2t-n) \tag{1}$$

$$\psi_i(t) = \sqrt{2}\sum_n H_b(n)\varphi_i(2t-n) \tag{2}$$

$$\varphi_r(t) = \sqrt{2}\sum_n L_a(n)\psi(2t-n) \tag{3}$$

$$\varphi_i(t) = \sqrt{2}\sum_n L_b(n)\psi_i(2t-n) \tag{4}$$

where L represents lowpass filters and H represents highpass filters. The wavelet functions ψ_r and ψ_i produce the complex wavelet function ψ_c, which is given by $\psi_r + j\psi_i$. The table of coefficients of the analyzing filters in the first level (Table1) and the remaining levels (Table 2) are given [14]. The coefficients of the synthesis filters are the transposes of the analysis filters.

Table 1. First level coefficients of the analysis filters

L_a	H_a	L_b	H_b
0	0	0.01122679	0
–0.08838834	–0.01122679	0.01122679	0
0.08838834	0.01122679	–0.08838834	–0.08838834
0.69587998	0.08838834	0.08838834	–0.08838834
0.69587998	0.08838834	0.69587998	0.69587998
0.08838834	–0.69587998	0.69587998	–0.69587998
–0.08838834	0.69587998	0.08838834	0.08838834
0.01122679	–0.08838834	–0.08838834	0.08838834
0.01122679	–0.08838834	0	0.01122679
0	0	0	–0.01122679

Table 2. Remaining levels coefficients of the analysis filters

LL_a	LH_a	LL_b	LH_b
0.03516384	0	0	–0.03516384
0	0	0	0
–0.08832942	–0.11430184	–0.11430184	0.08832942
0.23389032	0	0	0.23389032
0.76027237	0.58751830	0.58751830	–0.76027237
0.58751830	–0.76027237	0.76027237	0.58751830
0	0.23389032	0.23389032	0
–0.11430184	0.08832942	–0.08832942	–0.11430184
0	0	0	0
0	–0.03516384	0.03516384	0

#173666 - $15.00 USD Received 1 Aug 2012; revised 7 Nov 2012; accepted 9 Nov 2012; published 13 Nov 2012

In order to extend the transform to two-dimensional signals, a filter bank is applied separably in all dimensions. To compute the 2D DT-CWT of images the pair of trees are applied to the rows and then the columns of the image.

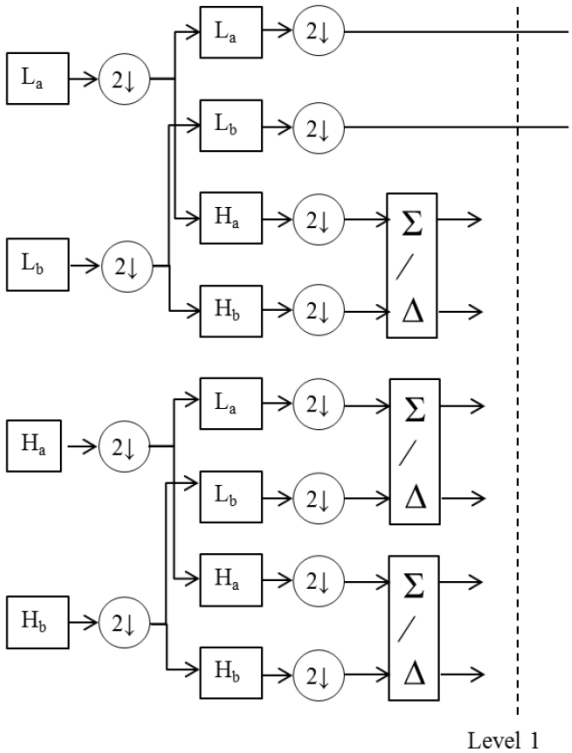

Fig. 1. Decomposition with 2D DT-CWT.

2D DT-CWT produces six high-pass subbands as well as two lowpass subbands at each level of decomposition (Fig. 1). In Fig. 1 [14], L represents lowpass filters and H represents highpass filters. Each filtering operation is followed by a downsampling by two. Six directional wavelets of DT-CWT are obtained by taking sum (Σ) and difference (Δ) of high-pass subbands which have the same pass bands.

As a result wavelets oriented at ±15°, ±45° ve ± 75° are obtained as [15]

$$1.\ (LH_a + LH_b)/\sqrt{2} \qquad 3.\ (HL_a + HL_b)/\sqrt{2} \qquad 5.\ (HH_a + HH_b)/\sqrt{2}$$

$$2.\ (LH_a - LH_b)/\sqrt{2} \qquad 4.\ (HL_a - HL_b)/\sqrt{2} \qquad 6.\ (HH_a - HH_b)/\sqrt{2}$$

Denoised image is obtained by performing inverse DT-CWT after modifying the wavelet coefficients according to some rules.

The DT-CWT gives a 4:1 redundancy for 2D images, this redundancy allows both shift invariance and good directional sensitivity.

2.2. Test images

In order to validate our method we used eleven test images (Fig. 2). Six of them are microscopic images that taken from Nikon and Olympus Fluorescence Microscopy Digital Image Gallery websites (Madin-Darby Canine Kidney Epithelial Cells, Mouse Kidney Tissue, African Water Mongoose Skin Fibroblast Cells, Tahr Ovary Epithelial Cells, Lily Flower Bud, Human Roundworm). Three of them are standard test images (Cameraman, Lena, Peppers) and one of them is Magnetic Resonance Image.

#173666 - $15.00 USD Received 1 Aug 2012; revised 7 Nov 2012; accepted 9 Nov 2012; published 13 Nov 2012

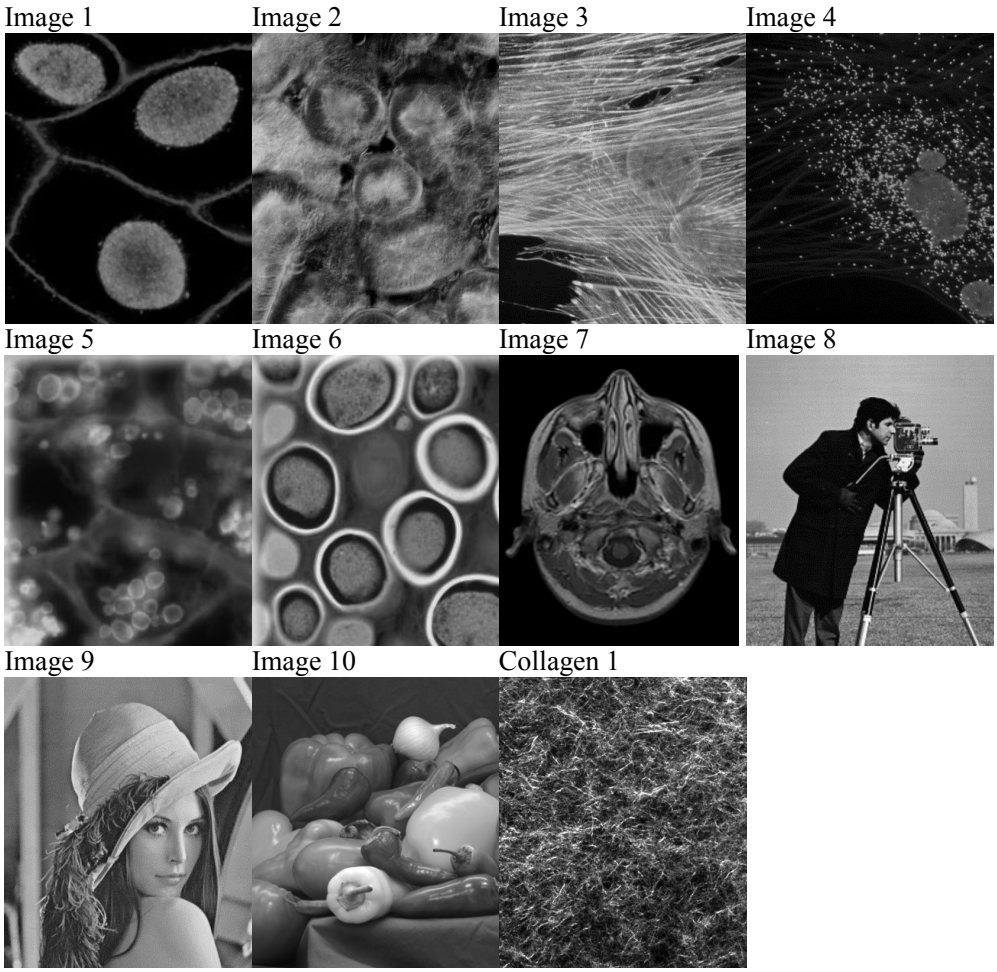

Fig. 2. Test images.

Additionally, in order to evaluate the performance of our algorithm on fibrillar structures in terms of contrast to noise ratio, we used Collagen I SHG (Second Harmonic Generation) image (UA Bimedical Eng. Lab.).

2.3. Proposed method

Firstly degraded image was decomposed using one level DT-CWT. Two approximation and six wavelet coefficients are obtained. Six complex wavelets are oriented in ±15°, ±45° and ±75° directions and captures image information in that direction. Our proposed method use the approximation coeffients at the same scale for the threshold value of wavelet coefficients. The threshold values for real and imaginary parts are calculated as:

$$T_{real} = 0.001 \times \sqrt{a_{r1}^2 + a_{r2}^2 + ...a_{rn}^2} \tag{5}$$

$$T_{imag} = 0.001 \times \sqrt{a_{i1}^2 + a_{i2}^2 + ...a_{in}^2} \tag{6}$$

where a_r and a_i represents real and imaginary parts of the approximation coefficients at the first level respectively.

#173666 - $15.00 USD Received 1 Aug 2012; revised 7 Nov 2012; accepted 9 Nov 2012; published 13 Nov 2012

Soft thresholding is applied separately to the real and imaginary parts of the wavelet coefficients.

$$\begin{cases} |x| > T \Rightarrow f(x) = \text{sgn}(x)(|x| - T) \\ |x| \le T \Rightarrow f(x) = 0 \end{cases} \tag{7}$$

where x represents noisy coefficients, T represents threshold value and $f(x)$ represents thresholded coefficients. After soft thresholding denoised image is obtained by performing inverse DT-CWT.

To validate the effectiveness of our proposed method, it is compared with Wavelet Packet Transform based soft thresholding denoising and a state-of-the art method called PURE-LET which is very efficient for the denoising of images corrupted by Poisson noise [9].

2.4. Image quality metrics

The performance of the proposed de-noising algorithm is quantitatively assessed using RMSE (Root Mean Square Error).

$$RMSE = \sqrt{\frac{1}{mn}\sum_{i=0}^{m-1}\sum_{j=0}^{n-1}\left[G(i,j) - F(i,j)\right]^2} \tag{8}$$

where G represents degraded image, F represents reference image and mn represents image size.

Test images were degraded artificially with Poisson noise. The RMSE values were calculated for images before and after the applications of the denoising methods (Table 3). Each of the algorithms was run 100 times, the mean and the standard deviation of the results were recorded.

Since the noise free reference image of Collagen is not known, image quality of Collagen assessed with CNR metric. CNR gives an objective measure of useful contrast between a region of background noise (reference) and an image feature (target) [16]. The CNR is used to determine whether the fibers become more apparent compared to the background after denoising with proposed method.

In order to calculate CNR four regions-of-interest (ROI) are defined in the image. Means and standard deviations of the image feature (region with fiber) and background (region without fiber) are calculated for each region.

$$CNR = 10\log\left(\frac{\mu_t - \mu_r}{\sqrt{\sigma_t^2 + \sigma_r^2}}\right) \tag{9}$$

where μ_t and σ_t represent the mean and standard deviation of the region of image feature; μ_r and σ_r represent the mean and standard deviation of the background noise [16].

3. Results

Since the main source of noise is Poisson Noise in optical imaging, in order to evaluate the performance of our algorithm test images were degraded artificially with Poisson noise. The performance of the de-noising methods are quantitatively assessed using RMSE. Our method gives less RMSE than other methods for all comparisons (Table 3).

PURE-LET produces visible edge artifacts due to aliasing. Our DT-CWT based method does not exhibit this phenomena, which can be seen in Fig. 3. Figure 3 shows a magnified part of the cameraman image.

The performance of the proposed de-noising algorithm on Collagen image is quantitatively assessed using CNR. Four ROIs were defined on the denoised and recorded

#173666 - $15.00 USD Received 1 Aug 2012; revised 7 Nov 2012; accepted 9 Nov 2012; published 13 Nov 2012

images (Figs. 4a, 4b). Figure 4b shows a sample ROI in the magnified part of the Collagen image.

Table 3. Comparison of proposed method with other methods in terms of RMSE

	Noisy Image	Proposed Method	PURE-LET	Wavelet Packet
Image 1	5.3612 ± 0.0326	3.6574 ± 0.0227	4.1202 ± 0.0222	4,3589 ± 0,0285
Image 2	9.6204 ± 0.0193	5.1791 ± 0.0147	6.2196 ± 0.0140	7,0941 ± 0,0180
Image 3	10.8999 ± 0.0210	7.7029 ± 0.0158	8.0599 ± 0.0163	8,6925 ± 0,0203
Image 4	5.5502 ± 0.0146	4.4969 ± 0.0136	4.7327 ± 0.0140	4,6577 ± 0,0151
Image 5	8.5834 ± 0.0263	4.2606 ± 0.0270	4.7496 ± 0.0194	5,7848 ± 0,0277
Image 6	10.0060 ± 0.0315	5.2560 ± 0.0235	6.9648 ± 0.0258	7,3135 ± 0,0242
Image 7	6.2529 ± 0.0334	4.3780 ± 0.0272	5.1844 ± 0.0284	5,0530 ± 0,0388
Image 8	10.8664 ± 0.0177	5.3306 ± 0.0125	5.7988 ± 0.0137	7,9143 ± 0,0153
Image 9	11.1375 ± 0.0168	6.2025 ± 0.0117	6.3451 ± 0.0136	8,1607 ± 0,0165
Image 10	9.4922 ± 0.0217	4.9888 ± 0.0198	5.4295 ± 0.0197	6,6924 ± 0,0244

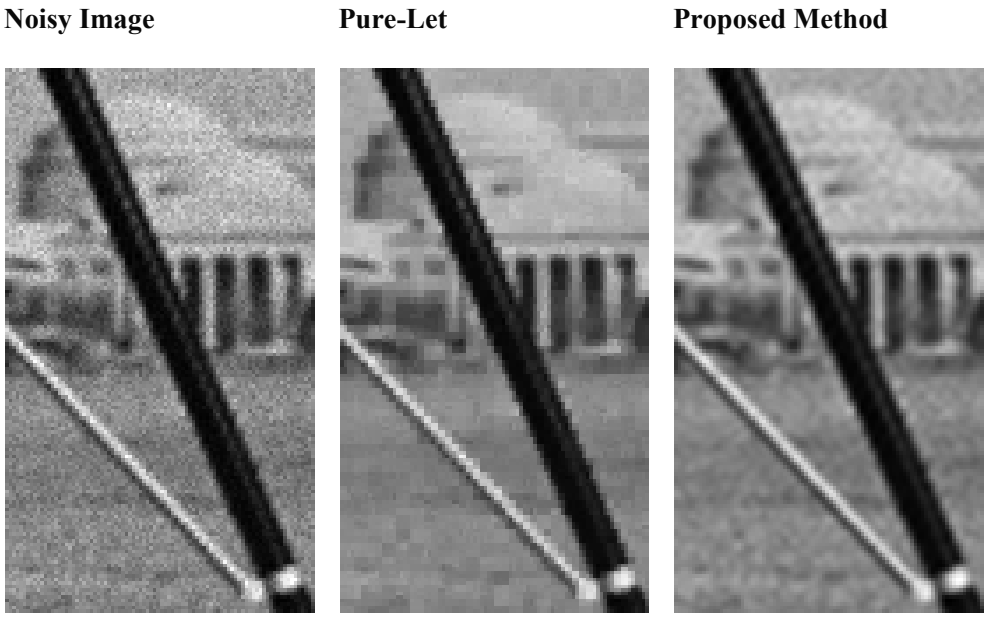

Fig. 3. Aliasing effect.

CNR values were averaged over four ROIs. As shown in Table 4 the average CNR improvement after denoising is about 61%. The collagen fibers become more apparent compared to the background.

The results show that the our approach leads to better denoising with well-preserved image details.

#173666 - $15.00 USD Received 1 Aug 2012; revised 7 Nov 2012; accepted 9 Nov 2012; published 13 Nov 2012

a.

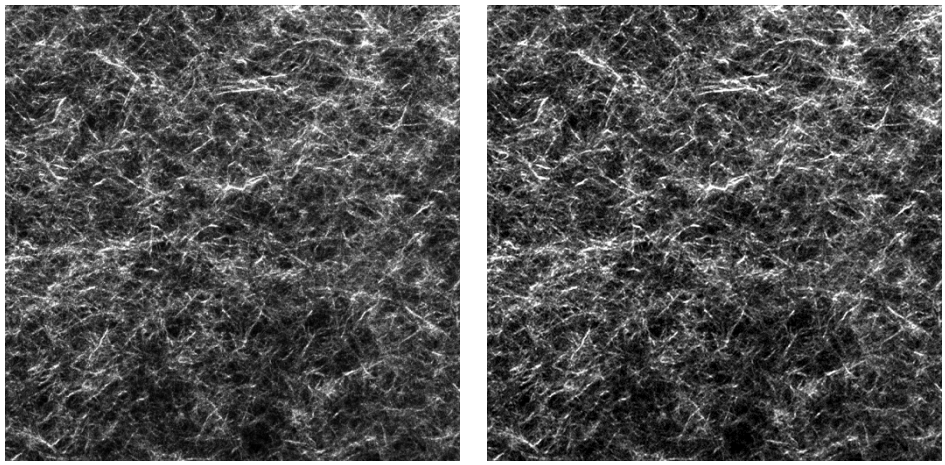

b.

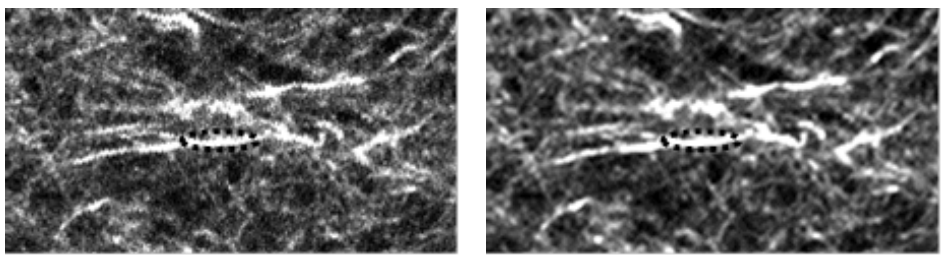

Fig. 4. (a) Collagen fiber image. (Left) Recorded image. (Right) Enhanced image using proposed method. (b) Image feature selection on magnified images.

Table 4. Contrast enhancement effect of proposed method on collagen fiber image

	Recorded Image	Proposed Method
ROI 1.	2,57	3,58
ROI 2.	0,65	4,01
ROI 3.	3,19	3,91
ROI 4.	2,98	3,66
Average CNR	2,35	3,79

4. Conclusion

Our proposed DT-CWT based denoising method results in less error than other methods for all test images corrupted by Poisson noise. In addition, proposed method significantly improves the contrast of images.

Since our method is not iterative and thresholding is applied to the wavelet coefficients obtained only after one level decomposition of image, it allows fast denoising. Optical imaging, especially time-series imaging, produce large amounts of data. Also optical imaging usually requires low light levels. Our proposed method allows fast and efficient enhancement of image stacks that obtained under low light intensity conditions.

#173666 - $15.00 USD Received 1 Aug 2012; revised 7 Nov 2012; accepted 9 Nov 2012; published 13 Nov 2012

DWT based denoising suffers from ringing and aliasing artifacts. Our DT-CWT based method does not produce these artifacts which can be explained by the shift invariance property and improved directional selectivity of DT-CWT.

The quality of the collagen fiber images from the TPLSM is poor. Therefore it would be desirable to have a method, which enhances the fiber structures in the image while reducing the noise substantially. Collagen fibers became more apparent compared to the background after denoising with proposed method. Our proposed method significantly improves the CNR while preserving the edges in the orientation of the fiber.

Acknowledgments

The author wishes to thank Dr. Urs Utzinger for allowing me use his laboratory equipment (UA Biomedical Eng. Lab) for the SHG imaging of Collagen I with the Two Photon Microscope.

#173666 - $15.00 USD Received 1 Aug 2012; revised 7 Nov 2012; accepted 9 Nov 2012; published 13 Nov 2012